Sensor Selection for Multiple Sensor Emitter Location Systems

Xi Hu and Mark L. Fowler
Dept. of Electrical and Computer Engineering
State University of New York at Binghamton
Binghamton, NY, USA 13902
{xhu1,mfowler}@binghamton.edu

Abstract—Multiple sensors can locate an emitter by sharing data between pairs of sensors and computing time/frequency-difference-of-arrival (TDOA/FDOA). We address optimal selection of a subset of sensors to reduce the needed network capacity. Fisher information is used to assess the data quality and geometric impact to manage the network to optimize the location accuracy subject to communication constraints.

We propose various approaches and discuss trade-offs. The first method assumes that the sensors have been pre-paired. The second method optimally determines pairings as well as selections of pairs but with the constraint that no sensors are shared between pairs. The third method consists of allowing sensors to be shared between pairs.

The first method is simple to solve but clearly the pre-pairing requirement makes this method very sub-optimal. In the second method, it is simple to evaluate the Fisher information but is challenging to make the optimal selections of sensors. However, the opposite is true in the third method: it is more challenging to evaluate the Fisher information but is simple to make the optimal selections of sensors.

TABLE OF CONTENTS

1. INTRODUCTION

Multiple sensors can locate an emitter by sharing data between pairs of sensors and computing time/frequency-difference-of-arrival (TDOA/FDOA). We address optimal selection of a subset of sensors to reduce the needed network capacity. Fisher information can be used to assess the data quality across multiple sensors to manage the network of sensors to optimize the location accuracy subject to communication constraints. From an unconstrained-resources viewpoint it is desirable to use the complete set of deployed sensors; however, that generally results in an excessive data volume. Selecting a subset of sensors to participate in a sensing task is crucial to satisfying trade-offs between accuracy and time-line requirements. For emitter location it is well-known that the geometry between sensors and the target plays a key role in determining the location accuracy. Furthermore, the deployed sensors have different data quality. Given these two factors, it is no trivial matter to select the optimal subset of sensors.

We propose various approaches to this problem and discuss trade-offs between them. The first method assumes that the sensors have pre-paired and share their data between these pairs; sensor selection then consists of selecting pairs to optimize performance while meeting constraints on number of pairs selected. The second method consists of optimally determining pairings as well as selections of pairs but with the constraint that no sensors are shared between pairs. The third method consists of allowing sensors to be shared between pairs.

We discuss several aspects of these three methods. The first method is simple to solve but clearly the pre-pairing requirement makes this method clumsy and very sub-optimal. In the second method, it is simple to evaluate the Fisher information but is challenging to make the optimal selections of sensors. However, in the third method things are reversed in that it is more challenging to evaluate the Fisher information but is simple to make the optimal selections of sensors.

Our general interest is in achieving network-wide optimization over a large number of simultaneously deployed sensors to enable more efficient and effective cooperation within the network of sensors.

We consider the specific scenario of using the sensors to locate a non-cooperative RF emitter by TDOA/FDOA-based methods; here TDOA refers to Time-Difference-of-Arrival and FDOA to Frequency-Difference-of-Arrival, which can be jointly estimated by cross-correlating signals from a pair of the sensors. The accuracy of the TDOA/FDOA estimates depends on the signal SNR and the time-frequency structure of the intercepted signal; however, the accuracy of the location estimation depends also on the emitter/sensor geometry. The goal of our work is to

[1] 1-4244-1488-1/08/$25.00 ©2008 IEEE.
[2] IEEEAC paper #1354, Version 3, Updated October 23, 2007

optimize over the set of all sensor assets, under the constraint of limited network communication resources.

2. PROBLEM DESCRIPTION

For simplicity we consider only the 2-D geometrical scenario. In the scenario we consider a rough estimate of emitter location has already been made (either by our system or by a cueing system). As shown in Figure 1, we wish to find the location of a stationary emitter, denoted by $\mathbf{u} \equiv [x_e, y_e]^T$, using signals intercepted at N unmanned aerial vehicle (UAV) sensors denoted S_1 to S_N, whose positions are $\mathbf{x}_i \equiv [x_i, y_i]^T$ and speeds are $\dot{\mathbf{x}}_i \equiv [\dot{x}_i, \dot{y}_i]^T$, for $i = 1, 2, \ldots, N$.

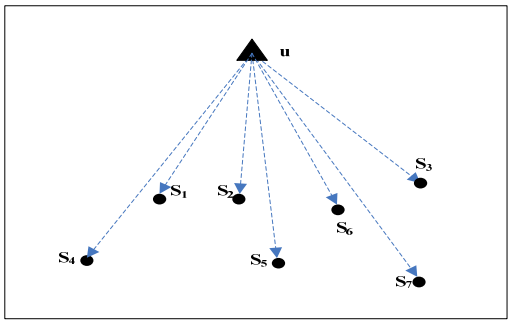

Figure 1 Geometry for stationary source location

Let r_i denote the Euclidean distance between the emitter and the i^{th} sensor S_i; that is

$$r_i = |\mathbf{x}_i - \mathbf{u}| = \sqrt{(x_i - x_e)^2 + (y_i - y_e)^2} \,. \tag{1}$$

To compute the TDOA/FDOA measurements the sensors must be paired. We consider three types of pairings within the network of sensors, as shown in Figure 2.

(1) Type-I: No Sensor Sharing (two pairs that do not share a sensor are said to be "independent pairs");

(2) Type-II: De-Centralized Sensor Sharing (i.e., sensors are shared between pairs but no sensor is part of more than two pairs);

(3) Type-III: Centralized Sensor Sharing (i.e., a common reference sensor is used).

For the i^{th} pair of sensors the TDOA τ_i and FDOA ω_i between the signals received at the two sensors in the pair are given by

$$\begin{aligned} \tau_i &= \frac{1}{c}\left(r_{i,1} - r_{i,2}\right) \\ \omega_i &= \frac{f_e}{c}\left(\mathbf{u}_{i,1}^T \cdot \dot{\mathbf{x}}_{i,1} - \mathbf{u}_{i,2}^T \cdot \dot{\mathbf{x}}_{i,2}\right), \end{aligned} \tag{2}$$

where $\mathbf{u}_{i.k}$ is the unit vector pointing from the k^{th} sensor in the i^{th} pair to the emitter, for $k = 1, 2$, and f_e is the transmitted frequency of the transmitter (assumed estimated in advance).

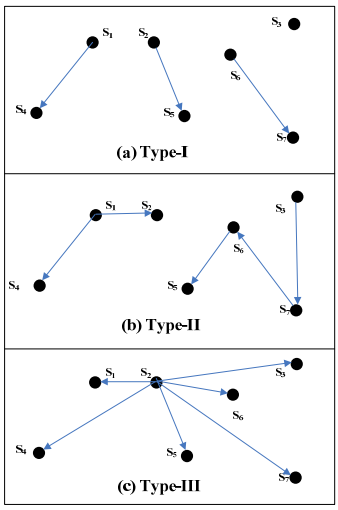

Figure 2 Three types of sensor network

Assume there are M pairs totally. Let $\boldsymbol{\theta}_m = [\tau_{k_m j_m}, \omega_{k_m j_m}]^T$ be the parameter vector to be estimated by the m^{th} pair of sensors, which is paired by $(k_m)^{th}$ and $(j_m)^{th}$ sensors, where $m = 1, 2, \ldots, M$; and $k_m j_m \in \{1, 2, ..., N\}, k_m \neq j_m$. Let $\hat{\tau}_{k_m j_m}$ and $\hat{\omega}_{k_m j_m}$ be the estimates, $\Delta\tau_{k_m j_m}$ and $\Delta\omega_{k_m j_m}$ be the estimation errors, then

$$\begin{aligned} \hat{\tau}_{k_m j_m} &= \tau_{k_m j_m} + \Delta\tau_{k_m j_m} \\ \hat{\omega}_{k_m j_m} &= \omega_{k_m j_m} + \Delta\omega_{k_m j_m} \end{aligned} \tag{3}$$

Because the estimate $\hat{\boldsymbol{\theta}}_m$ is obtained by maximum likelihood (ML) estimator [3], the asymptotic properties of ML estimators [4] gives that the PDF of it is Gaussian with covariance matrix that is the inverse of the Fisher information matrix (FIM), so

$$\begin{bmatrix} \Delta\tau_{k_m j_m} \\ \Delta\omega_{k_m j_m} \end{bmatrix} \sim N(0, \mathbf{FI}_m^{-1}) \tag{4}$$

As we know $\mathbf{FI}_m$ depends only on the sensors received signals according to [4]

$$\mathbf{FI}_m = 2\,\mathrm{Re}\left[\frac{\partial \mathbf{s}_m^H(\boldsymbol{\theta}_m)}{\partial \boldsymbol{\theta}_m}\boldsymbol{\Sigma}_m^{-1}\frac{\partial \mathbf{s}_m(\boldsymbol{\theta}_m)}{\partial \boldsymbol{\theta}_m}\right], \quad (5)$$

where $\mathbf{s}_m$ is the vector of received signals and $\boldsymbol{\Sigma}_m$ is the covariance of the AWGN at the m^{th} sensor pair. The FIM of $\boldsymbol{\theta} = [\boldsymbol{\theta}_1^T, \boldsymbol{\theta}_2^T, \ldots, \boldsymbol{\theta}_M^T]^T$ has a block structure as

$$\mathbf{F}_\theta = \begin{bmatrix} \mathbf{FI}_1 & \mathbf{I}_{12} & \cdots & \mathbf{I}_{1M} \\ \mathbf{I}_{21} & \mathbf{FI}_2 & \ddots & \mathbf{I}_{2M} \\ \vdots & \ddots & \ddots & \vdots \\ \mathbf{I}_{M1} & \mathbf{I}_{M2} & \cdots & \mathbf{FI}_M \end{bmatrix}, \quad (6)$$

where $\mathbf{I}_{m,k}$ is the cross term FIM between m^{th} and k^{th} pairs, which is evaluated in Appendix-A.

The TDOA/FDOA estimates are then used by the sensor system to estimate the location of the emitter. Because of the asymptotic properties of the ML estimator of TDOA/FDOA we can take the TDOA/FDOA estimates as Gaussian so that the FIM of the estimate of the geo-location is given by [6]

$$\mathbf{J}_{geo} = \left[\mathbf{G}_1^{\mathrm{T}}, \cdots, \mathbf{G}_m, \cdots, \mathbf{G}_M^{\mathrm{T}}\right]\mathbf{F}_\theta \begin{bmatrix} \mathbf{G}_1 \\ \vdots \\ \mathbf{G}_M \end{bmatrix}, \quad (7)$$

where $\mathbf{G}_m$ is the Jacobian matrix of the m^{th} pair of sensors, defined by $\mathbf{G}_m = \dfrac{\partial \boldsymbol{\theta}_m(\mathbf{u})}{\partial \mathbf{u}}$ and calculated by

$$\mathbf{G}_m = \begin{bmatrix} (\mathbf{x}_{k_m} - \mathbf{u})^T / r_{k_m} - (\mathbf{x}_{j_m} - \mathbf{u})^T / r_{j_m} \\ (\mathbf{x}_{k_m} - \mathbf{u})^T \dot{\mathbf{r}}_{k_m} / r_{k_m}^2 - (\mathbf{x}_{j_m} - \mathbf{u})^T \dot{\mathbf{r}}_{j_m} / r_{j_m}^2 - \dot{\mathbf{x}}_{k_m}^T / r_{k_m} + \dot{\mathbf{x}}_{j_m}^T / r_{j_m} \end{bmatrix}. \quad (8)$$

Our objective is to select an optimal subset of sensors and pair them as well. The criterion we used to make the decision is the trace of FIM of geo-location [6],[7] as

$$\max_{\text{all possible subset solutions}} \left\{ trace(\mathbf{J}_{geo}(\text{subset})) \right\} \quad (9)$$

In the following sections, we discuss sensor selection algorithms for the three network types.

3. ALGORITHMS

3.1 Pre-Paired Sensors

When sensors are pre-paired, we simply select pairs instead of sensors. The FIM $\mathbf{FI}_m$ and cross-FIM $\mathbf{I}_{m,k}$ are evaluated based on the paring and sensor sharing.

Type-I: No Sensor Sharing—When no sensor is shared the cross-FIMs $\mathbf{I}_{m,k}$ are zero. The $\mathbf{FI}_m$ are evaluated individually for each pair. Then $\mathbf{F}_\theta$ will have block diagonal structure as

$$\mathbf{F}_\theta = \begin{bmatrix} \mathbf{FI}_1 & \mathbf{0} & \cdots & \mathbf{0} \\ \mathbf{0} & \mathbf{FI}_2 & \ddots & \mathbf{0} \\ \vdots & \ddots & \ddots & \vdots \\ \mathbf{0} & \mathbf{0} & \cdots & \mathbf{FI}_M \end{bmatrix} \quad (10)$$

The problem of selecting K sensor pairs from N pairs is specified by

$$\max_{p_1,\cdots,p_N} \{trace(p_1(\mathbf{G}_1^T\mathbf{FI}_1\mathbf{G}_1) + \cdots + p_N(\mathbf{G}_N^T\mathbf{FI}_N\mathbf{G}_N))\} \quad s.t. \quad p_1 + \cdots + p_N = K < N, \quad p_i \in \{0,1\} \quad (11)$$

The solution of this was discussed in [7]: we simply select the *K* pre-paired sensor pairs that have the largest values of

$$trace\{\mathbf{J}_{geo,k}\} = trace\{\mathbf{G}_k^T\mathbf{FI}_k\mathbf{G}_k\}. \quad (12)$$

Type-II: De-Centralized Sensor Sharing—Here we treat sensors by sensor sets, where a sensor set is defined as a group of sensors which have no connections to sensors outside the group and do not have any independent pairs inside the group. For the sensor network in Figure 2 (b), the sets are defined as in Figure 3.

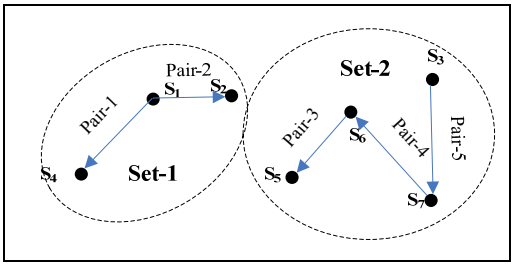

Figure 3 Sensor sets example

The geo-location FIM of each sensor set is computed; for example, the evaluation of set-1 is

$$\mathbf{J}_{geo,set-1} = \mathbf{G}_1^{\mathrm{T}}\mathbf{FI}_1\mathbf{G}_1 + \mathbf{G}_2^{\mathrm{T}}\mathbf{FI}_2\mathbf{G}_2 + 2\mathbf{G}_1^{\mathrm{T}}\mathbf{I}_{1,2}\mathbf{G}_2. \quad (13)$$

Then the problem of selecting K sensors from M sets is specified by

$$\max_{p_1,\cdots,p_N} \{trace(p_1 \cdot \mathbf{J}_{geo,set-1} + \cdots + p_M \cdot \mathbf{J}_{geo,set-M})\}$$
$$s.t. \quad p_1 \cdot n_1 + \cdots + p_1 \cdot n_M = K < N, \quad p_i \in \{0,1\} \quad (14)$$
$$n_i \text{ is the number of sensors in set-i}$$

and can be easily solved. For example, if we are asked to select 5 sensors, we can check the set which has 5 sensors, or the two sets which have 2 sensors and 3 sensors respectively, and add the trace of the two sets up, compare it with the one with 5 sensors and choose the larger one.

Type-III: Centralized Sensor Sharing—For the pre-paired case, the central sensor is already specified and the remaining $N-1$ sensors pair with it to form $N-1$ centralized pairs. There are C_{N-1}^{K} possible ways to select K pairs. The FIM of this set will have the following structure

$$\mathbf{J}_{geo,k} = \sum_{k=1}^{K} \mathbf{G}_k^{\mathrm{T}} \mathbf{F}\mathbf{I}_k \mathbf{G}_k + \sum_{m=1,k=m+1}^{m=K-1,k=K} 2\mathbf{G}_m^{\mathrm{T}} \mathbf{I}_{m,k} \mathbf{G}_k . \quad (15)$$

If the r^{th} sensor is the reference sensor then Appendix-A states that $\mathbf{F}\mathbf{I}_k = \mathbf{F}_k + \mathbf{F}_r$ and $\mathbf{I}_{m,k} \equiv \mathbf{F}_r$. In this case, we have to evaluate the trace of all the FIMs of geo-location of the C_{N-1}^{K} possible combinations, and choose the largest one:

$$\max_{set,k \in \{C_{N-1}^{K}\}} \{trace(\mathbf{J}_{set,k})\}$$
$$\{C_{N-1}^{K}\} \text{ is all the possible combination set} \quad (16)$$

3.2 Non-Pre-Paired Sensors

We are given a set of sensors and asked to optimally choose a subset and the optimal pairings as well. In this case the pairing provides more flexibility to enable better performance but it introduces additional complexity as well.

Type-I Pairing of Sensors: No Sensor Sharing—For N sensors, there could be $N/2$ independent pairs. To choose $K(\le N/2)$ pairs is a time-consuming work if we enumerated all the possible solutions. For example, $N=10$, there are $C_{10}^{2}=45$ possible pairs, and $(N-1)\cdot(N-3)\cdots 3\cdot 1 = 945$ possible ways to make 5 pairs as a subset. Fortunately, since there is no sensor sharing and we select sensors pair by pair, the selection of the next pair will not affect the selection of the previous one. This yields a tree structure and allows use of integer dynamic programming method [5]. For this paper we used the "Branch and Bound" method to choose a pair at each step. The objective function is

$$\max_{all\ feasible\ solutions} \left\{ \sum_{k=1}^{K} trace(\mathbf{J}_{geo,k^{th}\ pair\ in\ the\ solution}) \right\} \quad (17)$$

A "feasible solution" means any selection/pairing of sensors where no sensors are shared and the selected number of sensors is as required. Appendix-B illustrates a simple example of this method.

Type-II Pairing of Sensors: De-Centralized Sensor Sharing—For N sensors, there could be C_N^2 possible pairs. To choose $K(\le C_N^2)$ pairs, there are be $C_{C_N^2}^{K}$ possible ways to pair and then select K pairs. For example, for $N=10, K=5$, the number of ways is 122,1759, which is quite large and nonconductive to listing all of them. But fortunately, among all this large number of ways to pair and select, only a small number of them are unique. We have established the following theorem which is proved in Appendix-C.

Theorem: *For M sensors, at most independent $M-1$ pairs can be used as a "sensor set"; and different pairing methods of the M sensors to make $M-1$ independent pairs will result in the same CRLB of geo-location.*

We can exploit this result to simplify the optimal selection and pairing for this case. When we are given N sensors and asked to make K pairs, there are many solutions for this network. We can use at least $K+1$ sensors to make it or at most $2K$. Since the main advantage to share sensors is to save some sensor energies, we would like to use the number of sensors as less as possible. So here we only choose $K+1$ sensors to make K pairs.

For example, for given $N=7$ and $K=3$ pairs needed, compute the FIM of geo-location of all $C_7^4 = 35$ solutions, and find the one with the largest trace. Inside each solution, sensors are "paired by sequence." For example, as in Figure 4, the solution set is $\{S_4, S_1, S_2, S_5\}$.

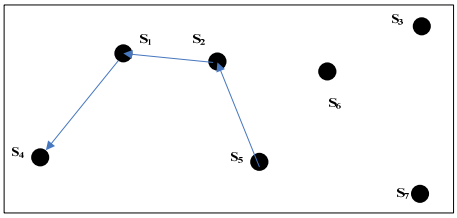

Figure 4 An example of pairing by sequence

4. SIMULATION RESULTS

To demonstrate the capability of the sensor selection methods we present some simulation results for the case of locating an emitter with a random lay-down of 14 sensors. The sensor selection proceeds as follows. Each sensor intercepts the emitter signal data at SNRs in the range of 10~15dB (where the SNR variation is assumed to depend quadratically on the range to the emitter). The full set of sensors share a very small amount of data to obtain a rough estimate of the emitter location; alternatively, we could consider the case where the system is cued by some other sensor system that provides a rough location that is to be improved using our sensors.

Figure 5 shows the performance of sensor selections without sensor sharing. We select 6 to 14 sensors to make 3 to 7 pairs, shown on the horizontal axis. The vertical axis shows the standard deviation of the geo-location error versus the number of sensors/pairs selected. The upper curve (-Δ-) shows the performance for the pre-paired sensor case without sharing; the lower curve (-O-) shows the performance when using the selection and pairing method discussed above for the case of no sensor sharing. Not surprisingly, the ability to select the pairing on the basis of the sensor geometry and the rough emitter location enables better performance than using pre-paired sensors.

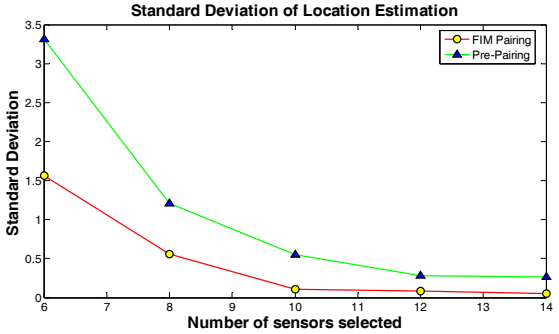

Figure 5 Performance of sensor selection w/o sharing

Figure 6 shows the time consumption used in pairing sensors for the non-sharing case versus the number of sensors/pairs selected. The upper line (-Δ-) shows the time required for the enumeration-based method, the lower one (-O-) shows the time required for our selection and pairing method. These time results are for matlab-based implementations.

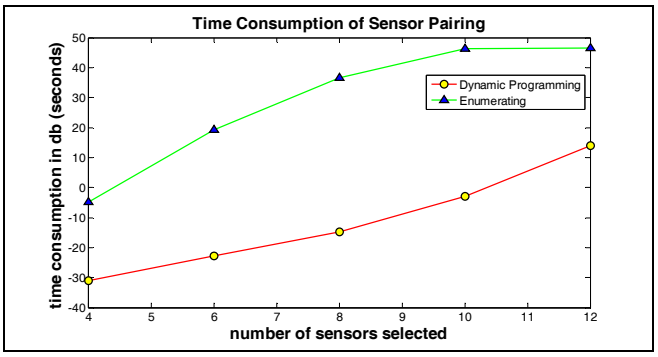

Figure 6 Time consumption of sensor pairing without sharing

Figure 7 shows the performance of sensor selections allowing sensor sharing. We select 5 to 11 sensors from 12, to make 4 to 10 pairs. It also shows the standard deviation of the geo-location error versus the number of sensors/pairs selected. The upper curve (-Δ-) shows the performance for the pre-paired sensor case with sharing; the lower curve (-O-) shows the performance using our selection and pairing method with sharing that is based on the Theorem in Section 3.2.

5. DISCUSSION

The results above show that it is possible to select and pair an optimal subset of sensors while significantly retaining performance levels. The sensor selection optimization problem was based on the fact that the geometry property and data quality of sensors play important roles in the emitter location estimation. We have used Fisher information to capture this inter-play between data quality and geometry. We have discussed different situations: (i) pre-paired sensors vs. optimally pairing the sensors, and (ii) allowing shared sensors or not. Following are some general conclusions made from this work.

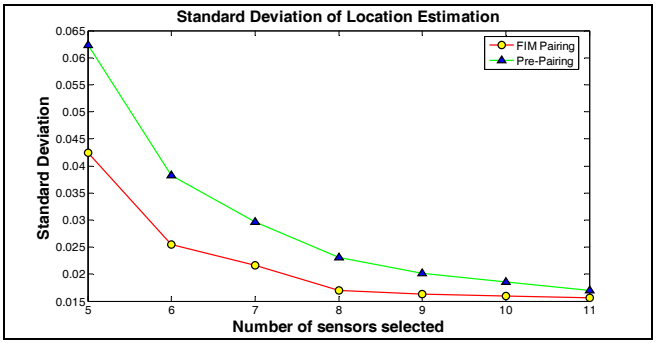

Figure 7 Performance of sensor selection allowed sharing

Conclusions: Without Sensor Sharing

- FIM of Geo-Location is easy to calculate, since each pair is independent;
- However, the pairing method is more complicated, since we need to consider all the possible paring ways;
- From a system point of view, the communication among different pairs can be done simultaneously;
- The number of pairs needed is small; beyond a certain point the accuracy improves slowly as more pairs are selected to participate.

Conclusions: With Sensor Sharing

- For a total of *N* sensors we can have as many as $N-1$ pairs, the more the higher accuracy of location estimation;
- Fortunately, FIM of all the possible independent sets are the same, so we do not need to consider about the pairing method. One simple way is to pair the sensors in nature order. This is the main result of this work and leads to a major reduction in the optimization processing required.
- However, since not all the pairs are uncoupled, there are cross terms in the TDOA/FDOA FIM. This complicates the computation required to support the optimization processing.
- Some sensors work in more than one pair, the communication among them needs to be considered carefully to avoid collision. This will be the focus of future work.

APPENDIX-A EVALUATION OF FIM CROSS-TERM

Consider the case where two pairs share one sensor, as shown in Figure 8.

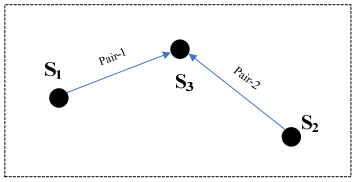

Figure 8 Two pairs shared one sensor

The three received signals at the sensors are

$$\begin{aligned} s_1[n] &= s[nT-\tau_1]e^{jv_1 nT}+\omega_1[n] \\ s_2[n] &= s[nT-\tau_2]e^{jv_2 nT}+\omega_2[n] \\ s_3[n] &= s[nT-\tau_3]e^{jv_3 nT}+\omega_3[n] \end{aligned} \tag{18}$$

where $s[nT]$ is the sampled transmitted signal, and $\omega_i[n], i=1,2,3$ is the AWGN received by sensor.

Let

$$\mathbf{s}=\begin{bmatrix}\mathbf{s}_1\\ \mathbf{s}_2\\ \mathbf{s}_3\end{bmatrix} \quad and \quad \tau_{13}=\tau_1-\tau_3;\quad \tau_{23}=\tau_2-\tau_3 \tag{19}$$

The cross term FIM between pair-1 and pair-2 can be evaluated as

$$\mathbf{I}_{1,2}\big|_{1,1}=\left(\frac{\partial \mathbf{s}}{\partial \tau_{1,3}}\right)^H \bullet \left(\frac{\partial \mathbf{s}}{\partial \tau_{2,3}}\right) \tag{20}$$

Since

$$\frac{\partial \mathbf{s}}{\partial \tau_{1,3}}=\begin{bmatrix}\frac{\partial \mathbf{s}_1}{\partial \tau_{1,3}}\\ \frac{\partial \mathbf{s}_2}{\partial \tau_{1,3}}\\ \frac{\partial \mathbf{s}_3}{\partial \tau_{1,3}}\end{bmatrix}=\begin{bmatrix}\frac{\partial \mathbf{s}_1}{\partial \tau_1}\cdot\frac{\partial \tau_1}{\partial \tau_{1,3}}\\ \mathbf{0}\\ \frac{\partial \mathbf{s}_3}{\partial \tau_3}\cdot\frac{\partial \tau_3}{\partial \tau_{1,3}}\end{bmatrix}=\begin{bmatrix}\frac{\partial \mathbf{s}_1}{\partial \tau_1}\\ \mathbf{0}\\ -\frac{\partial \mathbf{s}_3}{\partial \tau_3}\end{bmatrix} \tag{21}$$

also

$$\frac{\partial \mathbf{s}}{\partial \tau_{2,3}}=\begin{bmatrix}\frac{\partial \mathbf{s}_1}{\partial \tau_{2,3}}\\ \frac{\partial \mathbf{s}_2}{\partial \tau_{2,3}}\\ \frac{\partial \mathbf{s}_3}{\partial \tau_{2,3}}\end{bmatrix}=\begin{bmatrix}\mathbf{0}\\ \frac{\partial \mathbf{s}_2}{\partial \tau_2}\cdot\frac{\partial \tau_2}{\partial \tau_{2,3}}\\ \frac{\partial \mathbf{s}_3}{\partial \tau_3}\cdot\frac{\partial \tau_3}{\partial \tau_{2,3}}\end{bmatrix}=\begin{bmatrix}\mathbf{0}\\ \frac{\partial \mathbf{s}_2}{\partial \tau_2}\\ -\frac{\partial \mathbf{s}_3}{\partial \tau_3}\end{bmatrix} \tag{22}$$

Substitute (21) and (22) into (20), we get

$$\mathbf{I}_{1,1}^{(1,2)}=\left(\frac{\partial \mathbf{s}_3}{\partial \tau_3}\right)^H \bullet \left(\frac{\partial \mathbf{s}_3}{\partial \tau_3}\right) \tag{23}$$

This is exactly the FI of TDOA of sensor S_3's received signal. Following the same rule we get

$$\mathbf{I}_{1,2}\big|_{1,2} = \left(\frac{\partial \mathbf{s}}{\partial \tau_{1,3}}\right)^H \bullet \left(\frac{\partial \mathbf{s}}{\partial \nu_{2,3}}\right) = \left(\frac{\partial \mathbf{s}_3}{\partial \tau_3}\right)^H \bullet \left(\frac{\partial \mathbf{s}_3}{\partial \nu_3}\right) \quad (24)$$

$$\mathbf{I}_{1,2}\big|_{2,1} = \left(\frac{\partial \mathbf{s}}{\partial \upsilon_{1,3}}\right)^H \bullet \left(\frac{\partial \mathbf{s}}{\partial \tau_{2,3}}\right) = \left(\frac{\partial \mathbf{s}_3}{\partial \nu_3}\right)^H \bullet \left(\frac{\partial \mathbf{s}_3}{\partial \tau_3}\right) \quad (25)$$

$$\mathbf{I}_{1,2}\big|_{2,2} = \left(\frac{\partial \mathbf{s}}{\partial \nu_{1,3}}\right)^H \bullet \left(\frac{\partial \mathbf{s}}{\partial \nu_{2,3}}\right) = \left(\frac{\partial \mathbf{s}_3}{\partial \nu_3}\right)^H \bullet \left(\frac{\partial \mathbf{s}_3}{\partial \nu_3}\right) \quad (26)$$

Therefore the FIM cross-term between pairs is just the FIM of the shared sensor itself. The FIM of $\boldsymbol{\theta} = [\tau_{1,3}, \upsilon_{1,3}, \tau_{2,3}, \upsilon_{2,3}]^T$ is

$$\mathbf{J}(\boldsymbol{\theta}) = \begin{bmatrix} \mathbf{FI}_1 & \mathbf{I}_{1,2} \\ \mathbf{I}_{1,2} & \mathbf{FI}_2 \end{bmatrix} = \begin{bmatrix} \mathbf{F}_1 + \mathbf{F}_3 & \mathbf{F}_3 \\ \mathbf{F}_3 & \mathbf{F}_2 + \mathbf{F}_3 \end{bmatrix} \quad (27)$$

where $\mathbf{F}_i$ is the FIM of TDOA/FDOA of i^{th} sensor.

APPENDIX-B AN EXAMPLE OF BRANCH AND BOUND METHOD USED IN SENSOR PAIRING

Branch and Bound method is a widely used algorithm for efficiently finding the optimal solution of an integer optimization problem. It is based on the fact that the enumeration of integer solutions has a tree structure. It begins "growing" the enumeration tree by creating partial solutions called "buds." The quality of a bud is assessed using the "bounding function," which provides an optimistic estimate of the best value that the objective function could possibly obtain by extending from a given bud. The best complete feasible solution found at any stage of growth of the tree is called the incumbent; a feasible solution is one that satisfies any given constraints. A complete solution occurs at a "leaf" in the tree. Efficiency is obtained by pruning unfruitful branches of the tree by using a "bounding function." Buds are pruned if (i) further growth can not yield a better result than the incumbent (i.e., the bounding function value of the bud is inferior to the objective function value of the incumbent), or (ii) further growth can not yield any feasible solutions. The optimal solution is found when further growth can not occur. For our application a feasible solution is one for which no sensor sharing occurs.

Consider an example of the sensor pairing and selection for $N = 8$ sensors; there are 28 possible pairs. In this example we will arbitrarily assign values for the each pair so as to illustrate the typical operation. Our objective function is

$$\max_{\textit{feasible solution}} \left\{ \sum_{n=1}^{N/2} trace(FIM_{n^{th}\textit{ pair in a solution}}) \right\} \quad (28)$$

Here, feasible solution is the combination of sensor pair without sensor sharing. The bounding function used is

$$\max_{\textit{any solutions}} \left\{ \sum_{n=1}^{N/2} trace(FIM_{n^{th}\textit{ pair in a solution}}) \right\} \quad (29)$$

The solution in bounding function can be any combination of sensors, shared or non-shared. Let (*n*, *m*) represent the pairing of sensor-*n* and sensor-*m*. In the first step, without loss of generality, we choose as buds that are the pairs that include sensor-1. Figure 9 shows this first layer of buds. If we choose pair (1,2) as the first pair, then the bounding function value for it is 71 in this example, which leaves pairs (3,5)-(3,6)-(7,8) as the subsequent possible pairs. Since sensor-1 and sensor-2 are actually paired, we did not reuse them in the bounding function calculation at this node or any descendent nodes. From the bounding function value we know that the very best objective function value that we might have at a leaf node descended from (1,2) is 71. Since sensor-3 is shared between two pairs, this solution is not feasible, but at this stage it is retained because this infeasible solution is simply used to evaluate the bounding function for the feasible solutions that lie below this bud.

The first step of the tree is generated from the root node by enumerating all the possible pairs which have sensor-1. By evaluating the bounding function, we get our first incumbent (i.e., best feasible solution so far) as (1,5)-(2,4)-(3,6)-(7,8) , as incumbent=70; the buds that are shown exceeding this value can not be the incumbent because their bounding functions are computed based on infeasible solutions; however, they are retained to be grown further in hope that they may yield winning feasible solutions in the future. We now prune the pairs (1,6) and (1,8), because their bounding function values are smaller than the incumbent's.

Pruned nodes are indicated by a dashed border, the incumbent node is indicated by a bold solid border; nodes whose bounding function value is larger than the incumbent's but are based on infeasible solutions are shown by a non-bold solid border.

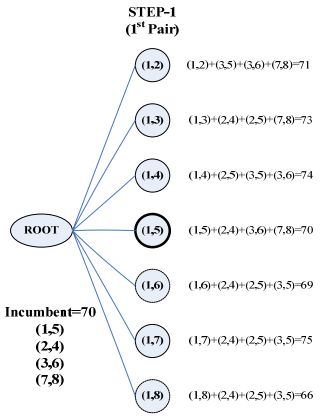

Figure 9: Illustration of first step of tree

There needs to be a policy that governs the choice of the next bud for expansion; we use the global-best node selection policy, which chooses from all the bud nodes on the tree the one that has the best value of the bounding function. Thus, we choose pair (1,7) , which has the largest bounding function value, for first further expansion. This gives the next tree step as shown in Figure 10.

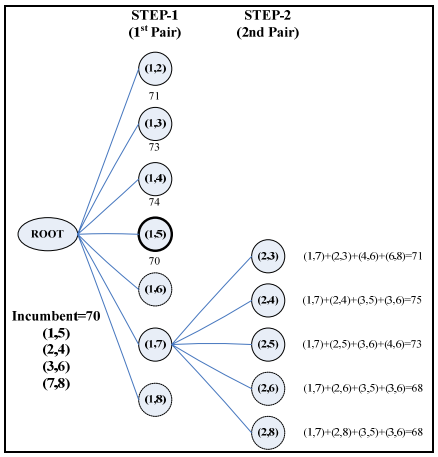

Figure 10: Illustration of second step in tree

This expansion is generated from the (1,7) node by enumerating all the possible pairs which have sensor-2, this is based on the so-called natural order. After evaluating all the bounding function values, some new nodes were pruned. But a new incumbent was not found in this expansion. Also, the global-best node selection policy assesses the bounding function values of all current remaining nodes (even those in the "Step-1 layer"), and chooses the one with the best bounding function value to expand further. Thus, the partial solution (1,7)-(2,4) is expanded next, which gives the result shown in Figure 11.

We now have found that (1,7)-(2,4)-(3,5) is a feasible solution with a value higher than the previous incumbent's value of 70 and higher than any other feasible bud; thus, it becomes the incumbent with a value of 74. Note that now all other remaining buds have bounding function values that are less than or equal to the incumbent's value of 74; therefore, it is impossible for any of these buds to generate a feasible solution that beats the current incumbent. Thus, all other nodes are shown as pruned in Figure 11, and (1,7)-(2,4)-(3,5)-(6,8) is the optimal feasible solution It should be noted that if all the buds grown out of (2,4) had a bounding function value less than the incumbent in Figure 10, then they would all be pruned; then the global-best node selection rule would go back to (1,4) and grow from there because it has the largest bounding function value of all buds grown so far on whole tree.

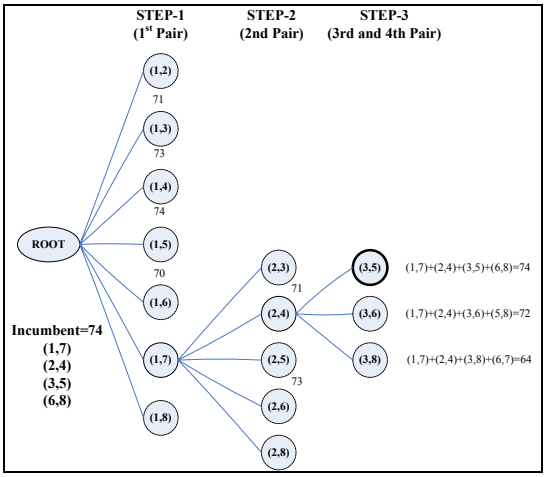

Figure 11: Illustration of third step in tree

In this particular example, we only evaluated 15 nodes, which is much smaller than the work of a full enumeration of the 105 possible solutions.

Simulation in Figure 12 gives the comparison of time consumption between enumeration method and the branch and bound method. We only let $N = 14$ for the largest number, since for larger N , the enumeration method is virtually impossible to realize.

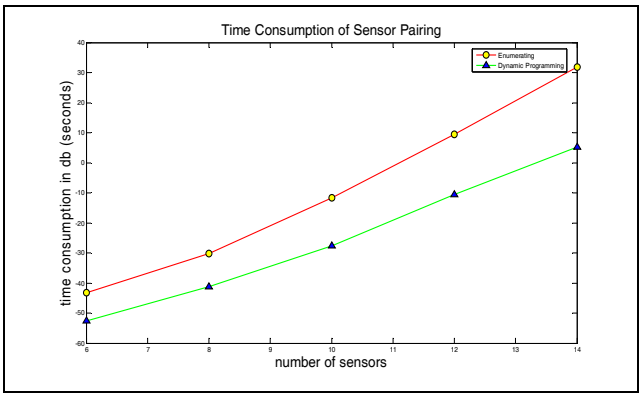

Figure 12 Time consumption of sensor pairing

APPENDIX-C PROOF OF THEOREM

Let r_k be the distance between S_k and the emitter and let $r_{k,j} = r_k - r_j$ be the sensor-emitter distance difference for $k, j \in \{1,2,...N\}, k \neq j$. Then the relations between r_k and $r_{k,j}$ are as following

$$\begin{bmatrix} r_{k_1 j_1} \\ r_{k_2 j_2} \\ \vdots \\ r_{k_M j_M} \end{bmatrix}_{M\times 1} = \mathbf{T}_{M\times N} \bullet \begin{bmatrix} r_1 \\ r_2 \\ \vdots \\ r_N \end{bmatrix}_{N\times 1} = \mathbf{T}\cdot\mathbf{r} \tag{30}$$

where $\mathbf{T}$ is an $M \times N$ matrix, (M is the number of pairs and N is the number of sensors), which has only one '1' and one '-1' in each row. For the structure of $\mathbf{T}$, the rank of $\mathbf{T}$ is less than $N-1$, which means there are at most $N-1$ r_{kj} independent pairs. Independent pairs, simply speaking, means that there are no closed loops in the graph of the sensors in the subset. For example, in the pairing in Figure 13, the pairs (1,2), (1,3) and (2,3) are dependent pairs; (3,4), (4,5) and (5,6) are independent pairs.

Let there be a different reference sensor (RS) in each different independent set as in Figure 14. In set-I, S_i is the RS; in set-J, S_j is the RS.

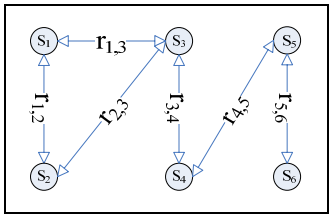

Figure 13 Independent and dependent pairs

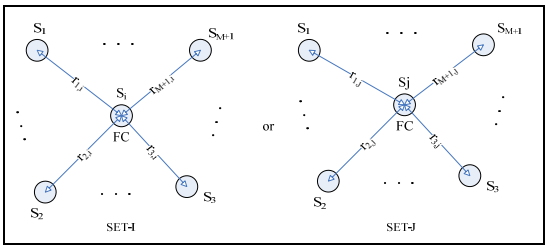

Figure 14 Same subset with different reference sensor

Let c be the signal propagation speed, the range difference equation is

$$r_{kj} = c\tau_{kj} = r_k - r_j \tag{31}$$

When the receivers are moving, taking time derivative of (31) yields a set of FDOA measurement equations

$$\dot{r}_{kj} = c\dot{\tau}_{kj} = \dot{r}_k - \dot{r}_j \tag{32}$$

where $\dot{r}_i$ is the rate of change of r_i. From the time derivative of (1), $\dot{r}_i$ is related to the unknown location $\mathbf{u}$ by

$$\dot{r}_i = \frac{(\mathbf{x}_i - \mathbf{u})^T \dot{\mathbf{x}}_i}{r_i} \tag{33}$$

Let $\mathbf{rd} = [r_1, r_2, \ldots, r_N, \dot{r}_1, \dot{r}_2, \ldots, \dot{r}_N]^T$, $\mathbf{p}_i = [r_{1i}, \ldots, r_{ki}, \ldots, r_{Ni}; \dot{r}_{1i}, \ldots, \dot{r}_{ki}, \ldots, \dot{r}_{Ni}]^T, k \neq i$ and $\mathbf{p}_j = [r_{1j}, \ldots, r_{kj}, \ldots, r_{Nj}; \dot{r}_{1j}, \ldots, \dot{r}_{kj}, \ldots, \dot{r}_{Nj}]^T, k \neq j$ then

$$\mathbf{p}_i = \begin{bmatrix} \mathbf{T}_i & \mathbf{0} \\ \mathbf{0} & \mathbf{T}_i \end{bmatrix} \bullet \mathbf{rd} = \mathbf{H}_i \bullet \mathbf{rd} \tag{34}$$

$$\mathbf{p}_j = \begin{bmatrix} \mathbf{T}_j & \mathbf{0} \\ \mathbf{0} & \mathbf{T}_j \end{bmatrix} \bullet \mathbf{rd} = \mathbf{H}_j \bullet \mathbf{rd} \tag{35}$$

where $\mathbf{T}_i$ and $\mathbf{T}_j$ are $(N-1)\times N$ matrixes, which only has one '1' and one '-1' in each row, and $\mathbf{0}$ is a $(N-1)\times N$ matrix with all 0 entries. It is easy to verify that there exists a $2(N-1)\times 2(N-1)$ full rank matrix $\mathbf{Q}_{ij}$, which satisfies

$$\mathbf{H}_j = \mathbf{Q}_{ij} \bullet \mathbf{H}_i \tag{36}$$

$$\mathbf{p}_j = \mathbf{H}_j \bullet \mathbf{rd} = \mathbf{Q}_{ij} \bullet \mathbf{H}_i \bullet \mathbf{rd} = \mathbf{Q}_{ij} \bullet \mathbf{p}_i \tag{37}$$

Then

$$\begin{aligned} CRLB(\hat{\mathbf{p}}_j) &= [\frac{\partial \mathbf{g}(\mathbf{p}_i)}{\partial \mathbf{p}_i}] \bullet CRLB(\hat{\mathbf{p}}_i) \bullet [\frac{\partial \mathbf{g}(\mathbf{p}_i)}{\partial \mathbf{p}_i}]^T \\ &= \mathbf{Q}_{ij} \bullet CRLB(\hat{\mathbf{p}}_i) \bullet \mathbf{Q}_{ij}^T \end{aligned} \tag{38}$$

Denote the emitter location $\mathbf{u}$ estimated by sensor pair set-I as $\hat{\mathbf{u}}_i$; then the CRLB of $\hat{\mathbf{u}}_i$ is

$$\text{CRLB}(\hat{\mathbf{u}}_i) = \mathbf{G}_i^T \bullet \mathbf{C}_i^{-1} \bullet \mathbf{G}_i \tag{39}$$

where $\mathbf{C}_i = E[\hat{\mathbf{p}}_i \cdot \hat{\mathbf{p}}_i^T]$ is the covariance matrix of the TDOA/FDOA estimates.

Since TDOA/FDOA are estimated by the ML method, we can assume that the covariance of the estimates achieve the CRLB, so $\mathbf{C}_i = CRLB(\hat{\mathbf{p}}_i)$ and

$$\mathbf{C}_j = CRLB(\hat{\mathbf{p}}_j) = \mathbf{Q}_{ij} \bullet CRLB(\hat{\mathbf{p}}_i) \bullet \mathbf{Q}_{ij}^T = \mathbf{Q}_{ij} \bullet \mathbf{C}_i \bullet \mathbf{Q}_{ij}^T \quad (40)$$

where $\mathbf{G}_i$ is the Jacobin matrix of set-I defined by

$$\mathbf{G}_j = \frac{\partial \mathbf{p}_j(\mathbf{u})}{\partial \mathbf{u}} = \frac{\partial}{\partial \mathbf{u}}[\mathbf{Q}_{ij} \bullet \mathbf{p}_i(\mathbf{u})] = \mathbf{Q}_{ij} \bullet \frac{\partial \mathbf{p}_i(\mathbf{u})}{\partial \mathbf{u}} = \mathbf{Q}_{ij} \bullet \mathbf{G}_i \quad (41)$$

Then

$$\begin{aligned} \mathrm{CRLB}(\hat{\mathbf{u}}_j) &= \mathbf{G}_j^T \bullet \mathbf{C}_j^{-1} \bullet \mathbf{G}_j \\ &= (\mathbf{Q}_{ij} \bullet \mathbf{G}_i)^T \bullet (\mathbf{Q}_{ij} \bullet \mathbf{C}_i \bullet \mathbf{Q}_{ij}^T)^{-1} \bullet (\mathbf{Q}_{ij} \bullet \mathbf{G}_i) \\ &= \mathbf{G}_i^T \bullet [\mathbf{Q}_{ij}^T (\mathbf{Q}_{ij}^T)^{-1}] \bullet \mathbf{C}_i^{-1} \bullet [\mathbf{Q}_{ij}^{-1} \mathbf{Q}_{ij}] \bullet \mathbf{G}_i \quad (42) \\ &= \mathbf{G}_i^T \bullet \mathbf{C}_i^{-1} \bullet \mathbf{G}_i \\ &= \mathrm{CRLB}(\hat{\mathbf{u}}_i) \end{aligned}$$

Thus, we have proved that for all the independent sets, the CRLB of emitter location estimation are the same.

REFERENCES

[1] D. J. Torrieri, "Statistical theory of passive location system," IEEE Transactions on Aerospace and Electronic Systems, vol. AES-20, no. 2, March 1984, pp. 183 – 198.

[2] P. C. Chestnut, "Emitter location accuracy using TDOA and differential doppler," IEEE Trans. Aerospace and Electronic Systems, vol. AES-18, March 1982, pp, 214-218

[3] S. Stein, "Differential delay/Doppler ML estimation with unknown signals," IEEE Trans. Signal Processing, vol. 41, August 1993, pp. 2717-2719

[4] S. Kay, Fundamentals of Statistical Signal Processing: Estimation Theory, Prentice Hall, 1993.

[5] N. Christofides, A. Mingozzi, P. Toth and C. Sandi, Combinatiorial Optimization, Wiley-Interscience, 1979

[6] M. L. Fowler and M. Chen, "Evaluating Fisher Information From Data for Task-Driven Data Compres-sion," Proceedings of Conference on Information Sciences and Systems, Princeton University, March 22-24, 2006, pp. 976 – 972.

[7] Xi Hu, Mo Chen, and M. L. Fowler, "Exploiting Data Compression Methods for Network-Level Management of Multi-Sensor Systems," Proceedings of SPIE - The International Society for Optical Engineering, v 6315, Mathematics of Data/Image Pattern Recognition, Compression, and Encryption with Applications IX, 2006.

BIOGRAPHY

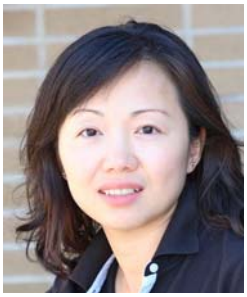

Xi Hu *was born in Shenyang, China. She received the B.Eng. in Electrical Engineering from Liaoning University, China in 1998 and the M.Eng. in Electrical Engineering in 2001 from Beijing Jiaotong University, China. She is currently a Research Assistant in the Department of Electrical and Computer Engineering at The State University of New York at Binghamton, where she is a Ph.D. candidate in Electrical Engineering. Her main research interests include estimation theory and data compression, with emphasis on sensor networks and in multiple sensor emitter location.*

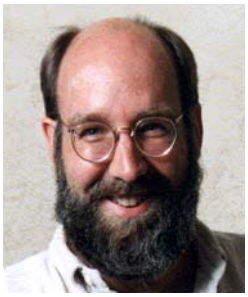

Mark Fowler *Mark L. Fowler received the B.T. in electrical engineering technology from the State University of New York at Binghamton in 1984 and the Ph.D. in electrical engineering from Pennsylvania State University, University Park, in 1991. Since 1999 he has been in the Department of Electrical and Computer Engineering at the State University of New York at Binghamton, where he is currently an Associate Professor. He is the director of the Emitter Location Research Group at Binghamton University. From 1991 to 1999 he was a Senior System Engineer at Lockheed Martin (formerly Loral (formerly IBM)) Federal Systems in Owego, NY, where he was responsible for algorithm development in the areas of emitter location systems. His research interests include data compression for sensor networks and remote sensing, TDOA/FDOA estimation, multi- and single-platform emitter location, frequency estimation, wavelet transform applications, and digital receiver techniques.*